energies

MDPI

Article

Optimizing Solar Parabolic Trough Receivers with External Fins: An Experimental Study on Enhancing Heat Transfer and Thermal Efficiency

Teerapath Limboonruang [1,*], Muyiwa Oyinlola [1], Dani Harmanto [1], Pracha Bunyawanichakul [2] and Nittalin Phunapai [2]

[1] Institute of Energy and Sustainable Development (IESD), De Montfort University, Leicester, United Kingdom.; muyiwa.oyinlola@dmu.ac.uk (M.O.); dani.harmanto@dmu.ac.uk (D.H.)
[2] Innovative Development, Automation System and Sustainability Laboratory (I-DASS Lab), Department of Mechanical Engineering, Faculty of Engineering, Srinakharinwirot University, Nakhornayok, Thailand.; prachabu@g.swu.ac.th (P.B.); nittalin@g.swu.ac.th (N.P.)
† This paper is an extended version of our paper published in 2022, International Conference on Heat Transfer, Fluid Mechanics and Thermodynamics (HEFAT-ATE 2022), Amsterdam, Netherlands, 8-10 August 2022; pp. 432-437.
* Correspondence: p2558151@my365.dmu.ac.uk; Tel.: +44 782 449 2049

Abstract: Several researchers have shown that increasing the surface area or internal fins improves the heat transfer performance of solar parabolic trough (SPT) receivers. However, the production of internally finned tubes has a difficult manufacturing process, resulting in significant cost increases. On the other hand, the addition of external fins to tubes is more technically and economically suitable for a low-resource setting. This study investigates the potential benefits of integrating external fins on the receiver of a low-cost SPT collector. Experiments were conducted using an SPT system with a focal length of 300 mm and a length of 5.1 m, combined with a sun tracking system. Experiments were run using smooth tubes and externally fins tubes, in each case at five different water flow rates. The results show that externally fins copper absorber tubes significantly enhanced the efficiency of the SPT collector system. The solar receiver with a fins tube was able to provide a maximum water temperature of 59.34 °C, compared with 56.52 °C for the smooth tube at 0.5 liters per minute. The externally fins solar absorber tube was found to have a maximum efficiency of 18.2% at an average daily solar intensity of 834.61 W/m^2, which is about 48% more efficient than the smooth tube.

Keywords: solar parabolic trough; solar energy; absorber tubes; renewable energy; fins tube

Citation: To be added by editorial staff during production.

Academic Editor: Firstname Lastname

Received: date
Accepted: date
Published: date

1. Introduction

The energy sector in Thailand depends heavily on imported oil and gas products. The current situation of dramatic increases in crude oil prices worldwide and the increased demand for energy have put the country in a tough economic situation and slowed down economic growth. Therefore, it is important to find alternative energy sources that guarantee security of supply. Solar energy has the greatest potential of all the sources of renewable energy [1-6], therefore, with the limited supply of fossil fuels, using solar energy has become inevitable. Thailand is located near the equator and has high potential for harnessing solar energy compared with other countries [7]. In fact, Thailand lies in high solar insolation band, where the average insolation intensity on a horizontal surface is approximately 1367 W/m^2 [3, 8] giving an enormous daily energy of 5 – 7 kWh/m^2/d, which is one of the highest in the world [3, 9, 10]. Thus, it presents an opportunity for energy independence and a better future for Thailand.

Solar thermal power plants with concentration technologies are important candidates for providing the bulk solar electricity needed within the next few decades [11, 12]. Solar collectors for high temperature require concentration systems, such as parabolic reflectors. Solar Parabolic Trough (SPT) has been proven to work, and they consist of large fields of parabolic trough collectors, a heat transfer fluid/steam generation system. A parabolic trough solar collector uses a mirror in the shape of a parabolic cylinder to reflect and concentrate the radiation from the sun towards a solar receiver tube located at the focus line of the parabolic cylinder [10, 13-15]. The solar receiver tube absorbs the incoming radiation and transforms it into thermal energy, the latter being transported and collected by a fluid medium circulating within the receiver tube. This method of concentrated solar collection has the advantage of high efficiency, and can be used either for thermal energy collection, for generating electricity [16] or for both, therefore it is an important way to exploit solar energy directly [17]. Furthermore, several studies have shown that concentrating solar plants have great prospects in terms of environmental impact and techno-economic factors [18-21]. For instance, India has avoided around 170,000 metric tons of CO_2e per year [19], while Pakistan has avoided over 225,000 metric tons of CO_2e per year [21]. The capital cost for parabolic collectors are quite high, for example, A 250 MW parabolic solar power plant in the United States costs $1.6 billion to build [22]. In Thailand [23], a huge budget of 900 million baht (estimated 30 million USD) is required for the construction of a 5 MW parabolic solar power plant. Therefore, it is important to explore opportunities to reduce costs such as developing local capacity and capability to innovate using local materials.

Several studies have been conducted to improve PTC performance, such as modifications of the geometry [24-29], enhancing the working fluids [30-32], introducing absorber tube coatings [33-35] , and tracker systems [36-38]. This study focuses on improving the thermal performance by modifying the geometry, specifically using the principle that the heat absorption of the solar receivers increases with an increase in the heat transfer area [28, 31]. A common method of modifying the geometry is by increasing the heat transfer area between the solar receiver tube and heat transfer fluid [39, 40] which results in better overall heat absorption. As a result, thermal enhancement is accomplished by manipulating properties, such as the system's geometry by adding artificial roughness [24-26], fins [27-29], baffles [41-43], wires [44-46], swirling devices [47-49] and vortex generators or by manipulating the material of the absorber tube [50-52] and fluid properties [32, 53, 54].

Several studies have shown internal fins can enhance the heat transfer. Huang, Yu [26] studied the effect of increasing the surface area inside the absorber tube by adding tubes with dimples or protrusions using computational simulation. Bellos, Tzivanidis [30] developed a fins absorber inside the tube to enhance thermal efficiency. Peng, Li [27] and Zhao, Bai [29] studied the impact of various fins shapes on the heat transfer and performance of solar absorber tubes. Improving a solar receiver tube by changing the geometry and adding an external fin enhances thermal efficiency. However, the manufacturing process of internal fin tubes is difficult and complicated, leading to higher production costs, especially in a low-income setting. Therefore, building on the principle that external fins will increase the surface area for absorbing solar radiation, this study experimentally examines the potential of using external fins to improve the thermal performance of a SPT. While the literature has many examples of internal fins, examples of external fins are limited, a few studies have used external fins such as, Gong, Wang [14] who used computational simulations to study the fins' shape in an absorber tube (AT) found that the thermal efficiency of the tube appeared to improve from 75.7% to 76.9% with the shorter, thicker AT fins, which increased heat transmission in the AT compared to the finless AT. However, thin, and long fins create more friction loss than wide and short fins due to the length of the tube. A computational study by Gong, Wang [13] has designed the AT by improving the hemispherical fins and the external fins with flat radiation shielding inside the evacuation ring for the PTC system. It was found that the optical and thermal efficiency

was 8% higher than the traditional one. Even though these computational studies show satisfactory performance results for externally fins absorber tubes, experimental studies are scarce in the literature. Furthermore, none of the previous studies included an economic and environmental assessment of a simple, low-cost manufacturing process. This study aims to fill this gap in the design and development of the solar parabolic trough collector system manufactured in Thailand. It achieves this by experimentally investigating the effects of external fins on the performance of absorber tubes. It provides insight into the temperature of the outflow water, heat transfer, and efficiency, as well as an evaluation of the economic and environmental aspects of the system.

2. Materials and Methods

2.1. Basic concept of Solar Parabolic Trough collector

The parabolic trough solar collector was constructed by using mirrors in the shape of a parabolic cylinder to reflect and concentrate solar radiation on an absorber tube located at the focal line of the parabolic cylinder. The absorber tube absorbs the incoming solar radiation and transforms it into thermal energy. A conceptual schematic of the design of the component of the parabolic shape [55] is shown in Figure 1.

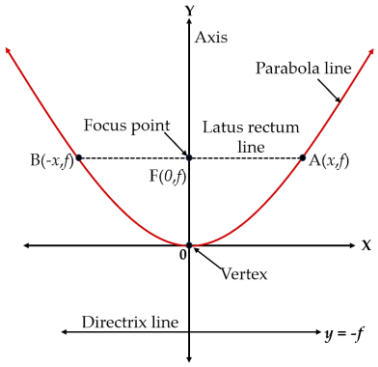

Figure 1. Basic concept of parabolic.

The equation for the parabolic trough in cylindrical coordinates is [56]:

$$y=\frac{x^2}{4f} \quad (1)$$

The reflector of a suitable parabolic design typically has focal length (f), to aperture width (W), ratio of about 0.25, as calculated from the equation [56]:

$$\frac{f}{W}=0.25 \quad (2)$$

The geometric concentration ratio (CR) of the parabolic trough collector is calculated from the following equation [57]:

$$CR=\frac{Aperture\ area}{Receiver\ area}=\frac{W\text{-}D_r}{\pi D_r} \quad (3)$$

The surface area of the solar receiver (A_r) tube is calculated from the equation:

$$A_r=\pi D_r L_r \quad (4)$$

Where D_r is receiver diameter and L_r is receiver length.

2.2. Basic earth-sun angles

On the basis of determining the position of point P on the earth's surface in relation to the solar radiation The parameters required for the design of a solar tracking system can be calculated at any instant by if the latitude (l), the hour angle (ω), and the sun's declination angle (δ) are known for that point, [8, 10, 55] as shown in Figure 2.

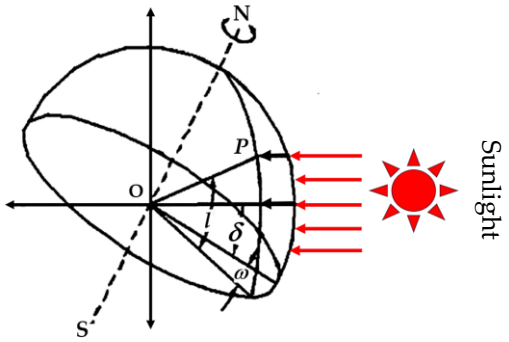

Figure 2. Latitude, hour angle and Sun's declination angles.

Declination Angle (δ) is the angular position of the sun at solar noon compared with the equator, which is between - 23.45°≤δ≤23.45°, computed from

$$\delta = 23.45sin\left(360\times\frac{284+n}{365}\right) \quad (5)$$

The angle of each hour (ω) obtained from

$$\omega = 15(12\text{-}st) \quad (6)$$

The local standard time (st) compared with the solar noon, an area test obtained from

$$st = Standard\ time+E\text{-}4\left(Long_{st}\text{-}Long_{Loc}\right) \quad (7)$$

2.3. *Experimental setup*

The experimental system described in Limboonruang et al. [55] was used to conduct the experiments. The Solar Parabolic Trough Collector (SPTC) system was set up with the long-axis of the parabola oriented along the north-south direction. The parabolic trough would therefore collect solar radiation in the east-west direction, as shown in Figures 3. The experimental system comprises three SPT, each measuring 1200×1520 mm² with a 300 mm focal length, which concentrate sunlight at the focal point. The components of the collector and solar parabolic trough assembly are as follows; (i) solar receivers vacuum tube; (ii) solar parabolic trough collector; (iii) solar hot water tank; and (iv) sun tracking system. The components of the system are arranged as shown in Figures 3 and 4; the solar tracking system for the SPT is as shown in Figure 5 and the characteristics of the SPT are shown in Table 1.

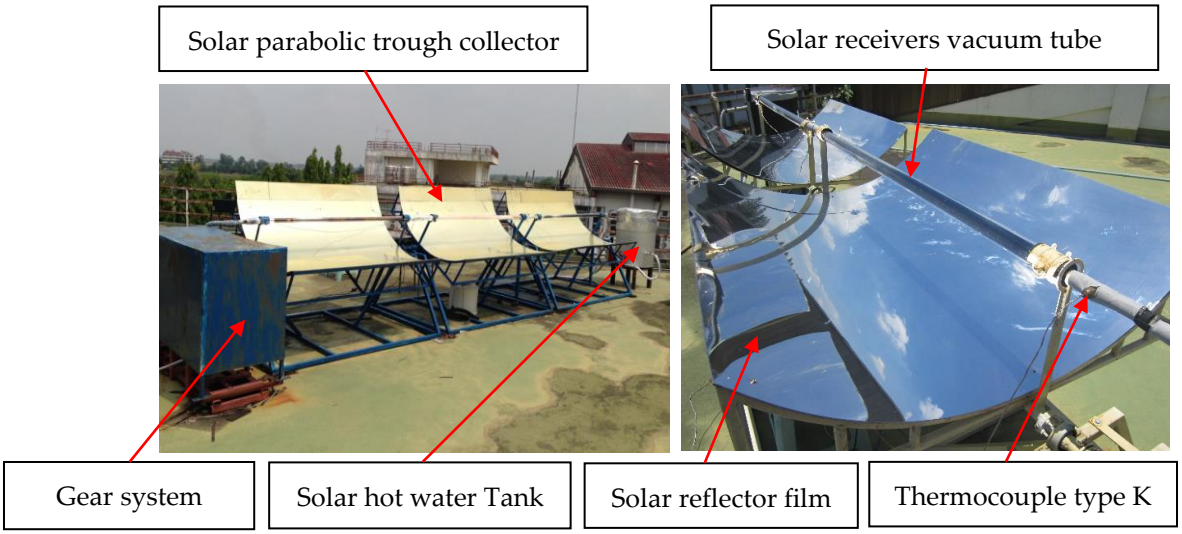

Figure 3. The Solar Parabolic Trough collector with solar tracking system [55].

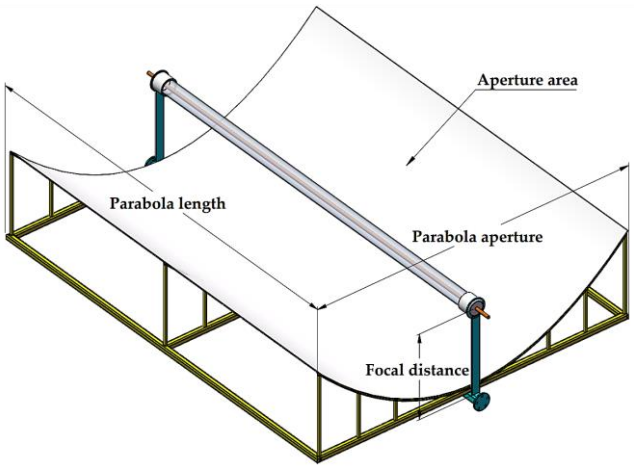

Figure 4. Schematic Diagram of the Solar Parabolic Trough Collectors (SPTC).

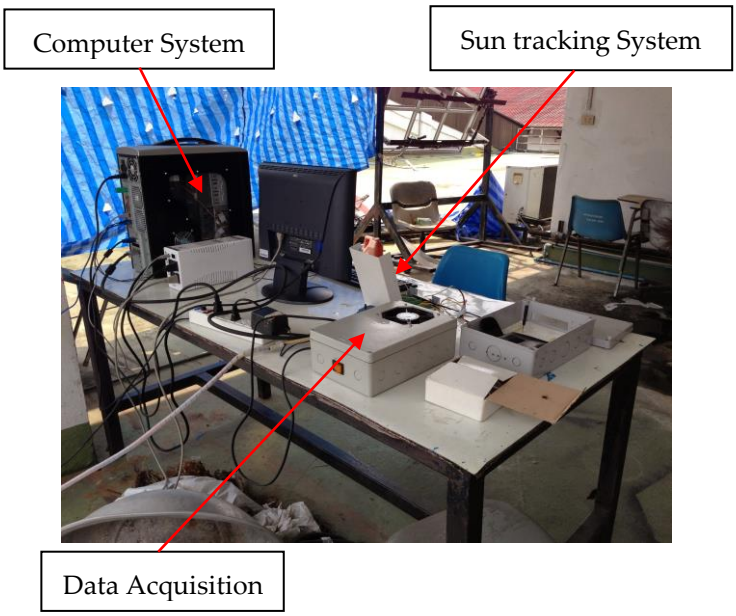

Figure 5. The Solar Tracking and Data Acquisition Systems for the SPT [55].

Table 1. Characteristics of each Solar Parabolic Trough Collector (SPTC) Set.

No.	Parameter	Characteristics
1	Parabola length (*L*)	1520 mm
2	Parabola aperture (*W*)	1200 mm
3	Focal distance (*f*)	300 mm
4	Thickness (mean value)	3 mm
5	Aperture area (A_a)	2.09 m²
6	Collector length (*L*)	1.52 m
7	Concentration ratio (*CR*)	8.13

The components and geometric parameters of the solar absorber vacuum tube assembly for the experiment as shown in Figure 6. Two types of absorber radiation were evaluated: 1) smooth copper tube, and 2) fins copper tube. The absorber tubes were mounted co-axially within an evacuated glass tube. The vacuum enclosure reduces thermal losses from the absorber tube. The design parameters of the tubes are shown in Table 2.

Table 2. Parameters of the solar receiver tube.

No.	Parameter	Volume/Type
1	Receiver material	copper
2	Receiver surface treatment	Heat resistant black coating
3	Inner copper tube diameter (D_{ci})	10 mm
4	Outer copper tube diameter (D_{co})	12.70 mm
5	Inner glass cover diameter (D_{gi})	33.50 mm
6	Outer glass cover diameter (D_{go})	47 mm
7	Glass envelope transmissivity	0.95
8	Receiver length (L_r)	1.52 m
9	Receiver area surface (A_r)	0.23 m²

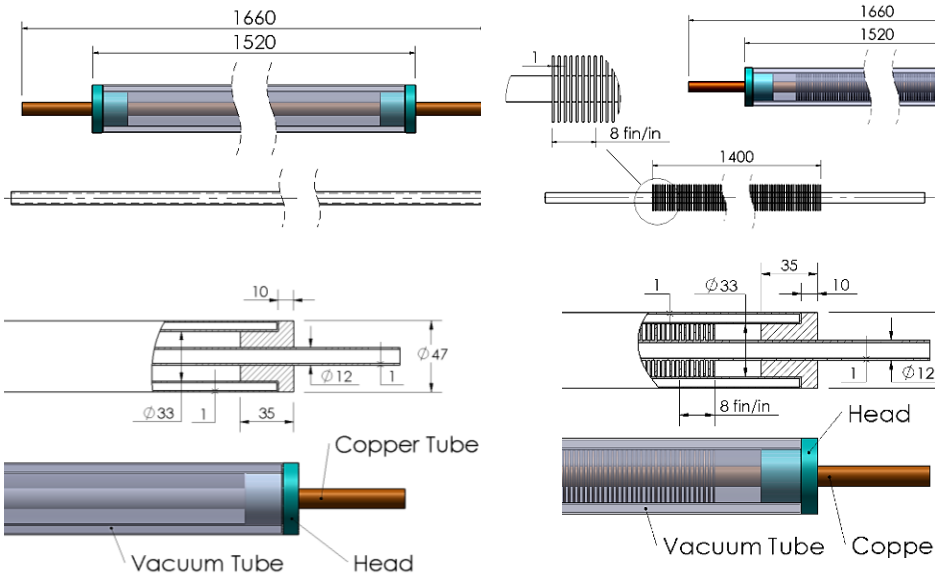

(**a**) (**b**) Unit: mm

Figure 6. Geometrical parameters of the solar receiver tube: (**a**) smooth copper tube; (**b**) fins copper tube.

The temperature of the circulating heat transfer fluid (in this case is water) was measured at the test points T_1 to T_4 on the absorber tubes and the local ambient air temperature was also measured (T_a). The distance between each measurement point T_1 to T_4 was 1.7 meters, as shown in Figure 7. The absorber tube's glass envelope has an external diameter of 47 mm. and an internal diameter of 33 mm. The copper absorber tube is mounted coaxially within the glass envelope and the envelope evacuated to help retain heat, as shown in Figure 8.

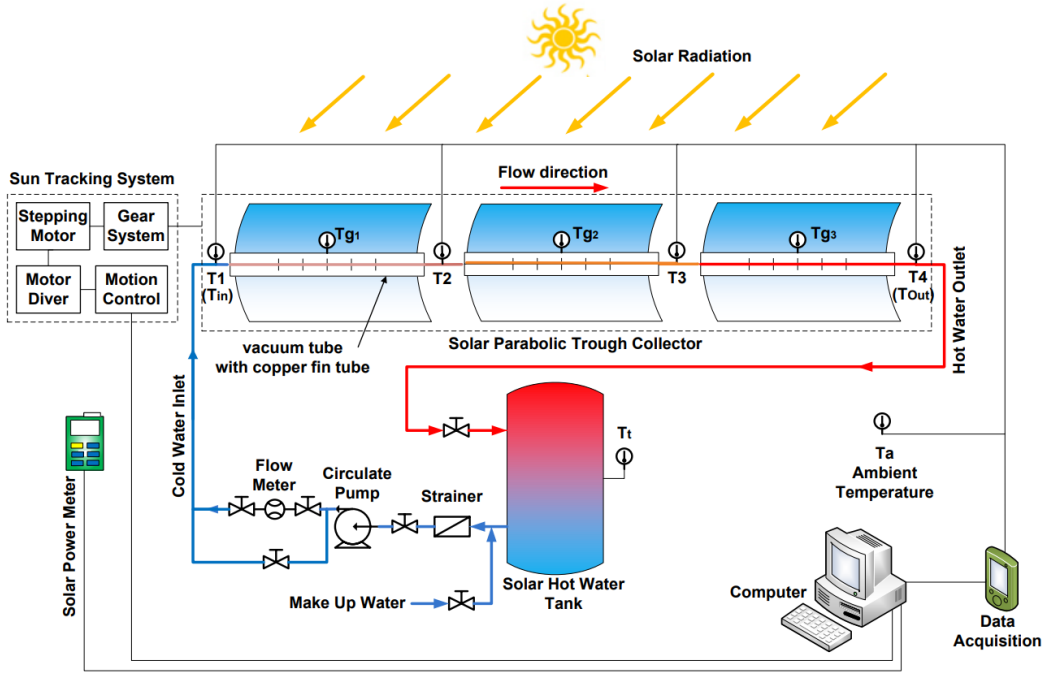

Figure 7. Schematic diagrams of experimental apparatus.

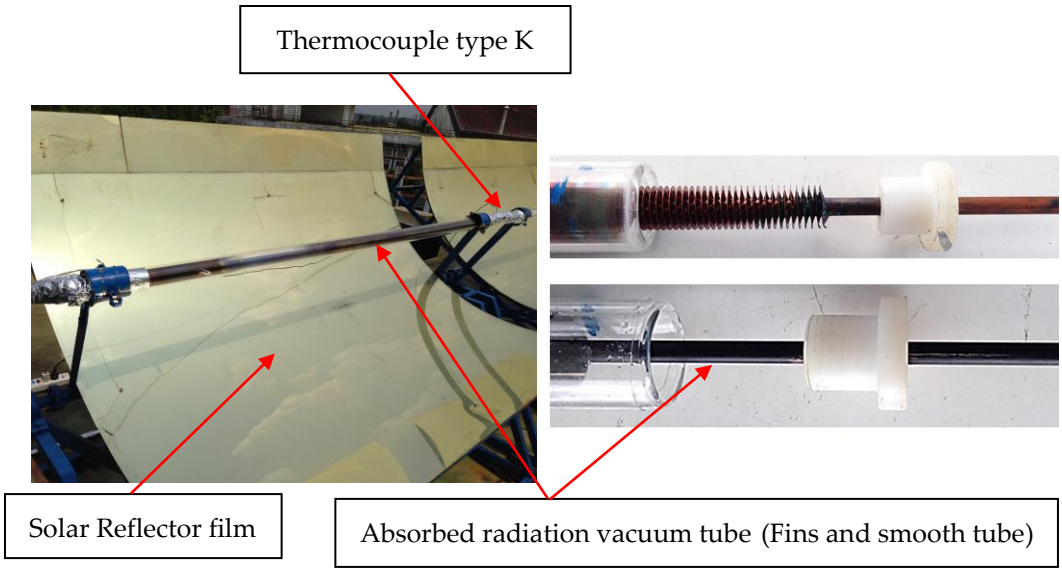

Figure 8. Absorber vacuum tube assemblies smooth and fins tube.

Experimental work was conducted by setting up the Solar Parabolic Trough Collector (SPTC) system with the long-axis of the parabola oriented along the north-south direction. The parabolic trough would therefore collect solar radiation along the east-west direction. The Heat Transfer Fluid (HTF) used in this experiment was water, supplied from a 60 liters storage tank. Water's physical properties are listed in Table 3. The controlled variable in the experiment was the flow rate of the water, specifically flow rates of 0.5, 1, 2, 3 and 4 liters per minute. Data collection was undertaken between the hours of 10:00-16:00 local time. The temperature at each test point (T_1 to T_4) and the air temperature (Ta) were measured using type-K thermocouples connected to a National Instruments NI-9213 data acquisition system and recorded every minute. A TES-1333R solar power meter, which has an accuracy of ±5% according to the manufacturer, was set up beside the SPT and was

used to measure the local direct solar light intensity (I_b) in units of W/m^2 once every minute. The flow rate was measured using a Well PRZ-15 flow meter which was connected to the piping system after the circulating pump and controlled the mass flow rate of the working fluid by adjusting the ball valve. The experiment was conducted over ten days in Nakhon-Nayok province, Thailand.

Table 3. Thermal properties of water at 25 °C.

No.	Parameter	Volume
1	Density (ρ)	997 kg/m^3
2	Boiling Point	100 °C
3	Specific Heat Capacity (C_p)	4180 J/(kg °C)
4	Dynamic viscosity (μ)	0.95×10^{-3} kg/m s
5	Thermal conductivity (k)	0.60 W/(m °C)

2.4 The Solar Tracking Systems

The SPT system is located in Nakhon Nayok Province, Thailand, at a longitude of 101.00° E and a latitude of 14.12° N. The time zone is UTC+07, and its proximity to the equator makes it strategically placed. During experiments, the SPT system was positioned with its parabolic trough's long axis aligned along the north-south direction. This positioning allowed the trough to collect solar radiation in the east-west direction throughout the experiment. The solar tracking system, shown in Figure 5, controlled the movement of the SPT unit. The solar tracking control system was created using LabVIEW version 2010 and based on equations (5)-(7), enabling the programming of position and time settings. The SPT was initially oriented east as the starting position. To start the program, the user must input the location, time zone, and local time into the software. Once these settings are in place, the program is ready to operate. The system then tracks the daily trajectory of the sun by rotating the SPT axis from east to west at a constant speed of 0.00415 degrees per second, using a stepping motor (ORIENTAL model PH599-A) connected to a gearbox designed for a total rotation of 15 degrees per hour [56]. At the end of the day, the SPT returns to its original position.

The experiment was conducted in Thailand from March 11 to 30, during the summer season. This corresponds to day numbers (n) 70 to 89 for the year. Using equation (5), the declination angle (δ) of the sun was calculated to be between -4.41° and 3.22°. Equation (8) [56] illustrates the angle of incidence for the SPT on a north-south axis with a continuous east-to-west trajectory. The resulting calculation shows an angle of $0.997 \le \cos\theta \le 0.998$.

$$\cos\theta = \cos\delta \quad (8)$$

Where θ is the sun's incident angle and δ is the sun's declination angle.

The concentrating solar system involves a horizontal single-axis solar tracking control system. As a result, the incident angle of the sun (θ) has an impact on the aperture area's effective daylight area (A_a). This is demonstrated in Figure 9. To calculate the effective intensity of sunlight falling on the collection area, it is important to take into account the solar intensity on the aperture area and the variable angle of incidence due to seasonal changes. This can be done using equation (9) [58].

$$I_{eff} = I_b \cos\theta \quad (9)$$

Where I_{eff} is the effective intensity of sunlight falling on the collection area, I_b is the local direct solar light intensity, and θ is the sun's incident angle. Based on the above findings, the effect of solar radiation is $0.997I_b \le I_{eff} \le 0.998I_b$, indicating a close resemblance to direct solar radiation. Therefore, we will use $I_{eff} \approx I_b$ to simplify calculations in this experiment.

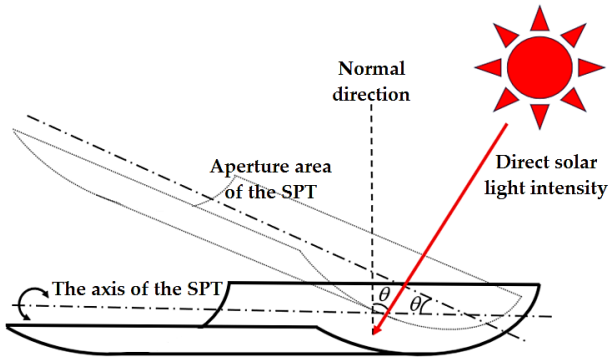

Figure 9. The effect of the angle of incidence of the sun on the aperture area.

2.5 Data Reduction

Average hourly data from all instruments were computed and used for analysis. The equations and the parameters used to calculate the data to determine the values used are summarized in Table 4.

Table 4. Details of data reduction.

Parameter	Relation	Units	Equation No
Mean glass receiver tube temperature	$T_g = \frac{\sum_{i=1}^{n} T_{gi}}{n}$	°C	(10)
The mean fluid temperature [28]	$T_{fm} = \frac{T_1 + T_4}{2}$	°C	(11)
Solar energy on the trough aperture [59]	$Q_s = \alpha A_a I_b$	W	(12)
Heat absorbed	$Q = \dot{m} C_p (T_4 - T_1)$	W	(13)
Daily energy gained by water [60]	$Q_{water} = mC_p(T_{final} - T_{initial})$	kJ	(14)
Overall efficiency	$\eta = \frac{\dot{m} C_p (T_{final} - T_{initial})}{\alpha A_a I_b}$	-	(15)
Water velocity	$v = \frac{\dot{V}}{A_c}$	m/s	(16)
Reynolds number	$Re = \frac{\rho v D_{ci}}{\mu}$	-	(17)

2.6 Economic Evaluation

The financial cost and revenue analysis of the SPT system was analyzed using the initial project cost and net present cost (C_{NPC}). This was used to determine the economic viability of the SPT system in order to estimate the project value by analyzing the investment value. This includes the project's payback period (*PB*), net present value (*NPV*), and internal rate of return (*IRR*).

The net present cost (C_{NPC}) can be calculated using equation (18) [61].

$$C_{NPC} = \frac{C_{TALC}}{CRF(i,N)} \quad (18)$$

Where C_{TALC} is the total annualized cost (*USD/year*), and *CRF(i, N)* is the capital recovery factor for the STP system for this case study, which can be calculated (19) [61].

$$CRF(i, N) = \frac{i(1+i)^N}{(1+i)^N - 1} \quad (19)$$

Where *N* is the product's lifetime (*year*) and *i* is the actual interest rate (%).

The net present value (*NPV*) can estimated using equation (20) [62, 63].

$$NPV=\sum_{i=1}^{n}\frac{R_i}{(1+r)^i}\text{-}Initial\ investment \quad (20)$$

Where R_i is the cash flow for *i* period, n is the life of the SPT system project (year) and *r* is discount rate, and The Internal Rate of Return (*IRR*) can be shown as follow in equation (21) [62, 63].

$$\sum_{i=1}^{n}\frac{R_i}{(1+IRR)^i}\text{-}Initial\ investment=0 \quad (21)$$

To estimate the payback period (*PB*), one must know the initial investment and the duration of the asset's expected cash flow. The following formula (22) [62, 63]is used to calculate.

$$PB=\frac{Initial\ investment}{Expected\ annual\ cash\ inflow.} \quad (22)$$

2.7 Uncertainty analysis

This section presents the experiment's inherent uncertainties. The solar power meter, type K thermocouples, flow meter, and data acquisition are used to collect the various types of data from the experiment. The standard uncertainty (F_z) of the parameters in the data calculation can be computed from equation (23), where Y_z is the accuracy of the devices [64] and the uncertainty $X_{(b)}$ can be computed using equation (24) [64].

$$F_Z=\frac{Y_Z}{\sqrt{3}} \quad (23)$$

$$X_{(b)}=\sqrt{\begin{matrix}\left(Uncertainty\ of\ Solar\ power\ meter\right)^2+\left(Uncertainty\ of\ Thermocouple\right)^2+\\ \left(Uncertainty\ of\ Flow\ meter\right)^2+\left(Uncertainty\ of\ Data\ logger\right)^2\end{matrix}} \quad (24)$$

Table 5 provides the devices' accuracy and uncertainty. As a result, the overall uncertainty error for the current experiment is 3.06%.

Table 5. Accuracy and uncertainty of measuring.

Instrument	Units	Range	Accuracy (%)	Uncertainty (%)
Solar power meter	W/m²	0-2000	±5	±2.886
Thermocouple Type-K	°C	-270 to 1260	±0.75	±0.433
Flow meter	Liters per minute	0.0 to 4.0	±1.6	±0.924
Data logger acquisition	°C	-	<0.02	±0.011

3. Results and discussion

This experiment aims to compare the thermal performance of absorbers with external fins tubes to smooth tubes in the SPT. The primary variable studied in this experiment is the flow rate of the heat transfer fluid in both fins and smooth copper absorber tubes.

3.1. Solar radiation with time

Figure 10 shows the variation of solar radiation with time. The experiment was done over 20 days. However, only the data from the 10 days with the least cloudiness was selected. All experimental data for the solar radiation data on a clear and cloudy day are shown in Figure A1. For this research, the data used was collected for 20 days, as shown in Figure 10. It is pertinent to note that on all days, the total amount of solar energy received by the collector was almost identical. As expected, solar radiation is time

dependent with a sharp rise between 10:00 and 11:00 am. During the morning period, solar radiation ranged from 474.45 to 1127.84 W/m², reaching a maximum between 11:00 and 13:00, and then begins to fall from 13:00 to 16:00. The average solar radiation observed was 834.61 W/m² over the 10 days of the experiment. This solar radiation profile is typical for around 8-10 months yearly in Thailand [65, 66], illustrating that PTC will perform well. However, in practical applications, the measured solar power values can vary over time due to uncontrollable factors such as cloud cover, wind, pollution, and atmospheric dust. These factors can all result in a decrease in the fraction of solar irradiation on the collector.

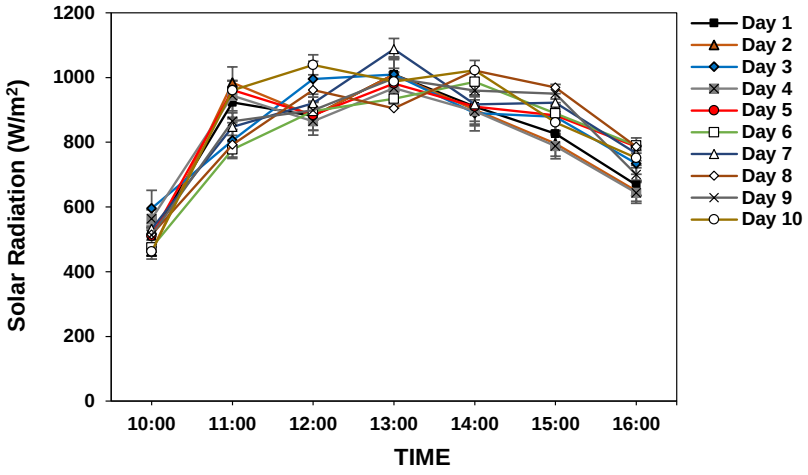

Figure 10. Variation of solar radiation with time.

3.2. Outlet water temperature

Figure 11 shows the effect of varying the flow rate of the water in the smooth and fins copper absorber tubes. Data was obtained by running the experiments at different flow rates, ranging from 0.5 to 4 liters per minute. As expected, the fluid outlet temperature decreases with an increase in flow rate, and it can be observed that the fins tubes consistently provide a higher outlet temperature than smooth tubes at the same flow rate. It can be seen to achieve a maximum outlet temperature of 56.52 °C at 0.5 liters per minute for a smooth tube and a maximum outlet temperature 59.34 °C at 0.5 liters per minute for a fins tube. The average daily ambient air temperature was 38.20 °C. Therefore, the results have shown the effect of mass flow rate and temperature difference. Higher temperature differences are from lower mass flow rates because working fluid in the tubes spends a longer time receiving energy at the lower water velocity. As the primary function of the SPT collector is to provide heat, running the collector at a lower flow rate is more beneficial in terms of higher outlet temperatures. Furthermore, because a lower flow rate implies a reduced pumping power requirement, the overall efficiency improves, as shown in a prior study [67, 68]. However, a solar receiver at a higher temperature implies a higher rate of heat loss from the solar absorber. As indicated in previous studies [28, 69], heat loss can be reduced by installing insulation on the solar receiver's surface, which will decrease the temperature of the solar receiver and minimize the overall heat loss.

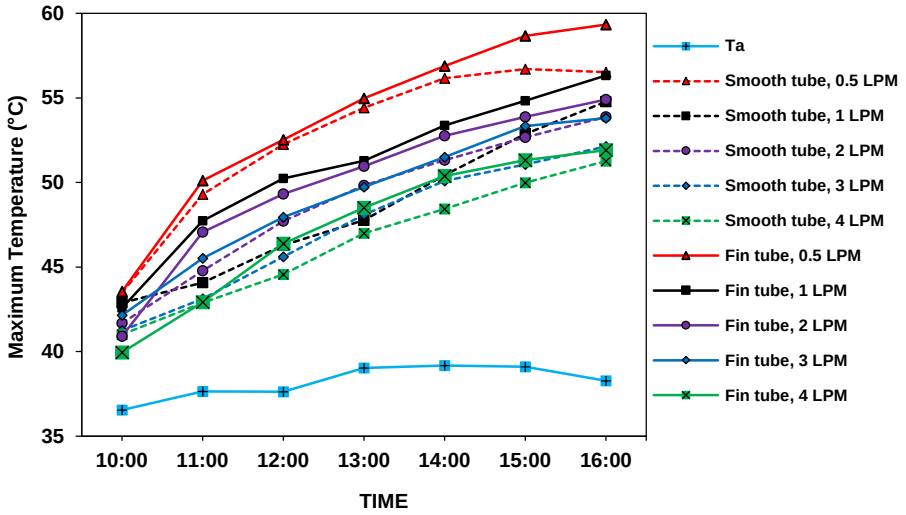

Figure 11. Comparison of outlet water temperature with time at various flow rates for smooth and fins tubes.

Figure 12 shows the smooth and fins copper absorber tubes' maximum output water temperature as a function of the water flow rate, and Table 6 compares outlet water temperatures for smooth and fins tubes. It can be observed that externally finned copper tubes deliver higher temperatures than smooth copper tubes at all flow rates studied. With a flow rate of 0.5 liters per minute, the maximum output temperature from the fins tube is 59.34 °C, this is 2.82 °C more than for the smooth copper pipe, representing a 4.75% increase. When the flow rate was increased, the output temperature was observed to decrease for both types of tube. It should be noted, some abnormal data shown in Figures 11 and 12 was due to the occasional passing of clouds and wind in the atmosphere, which can cause decreases in solar intensity. It affected the outlet water temperature. However, these graphs' trends returned to normal after the clouds moved through.

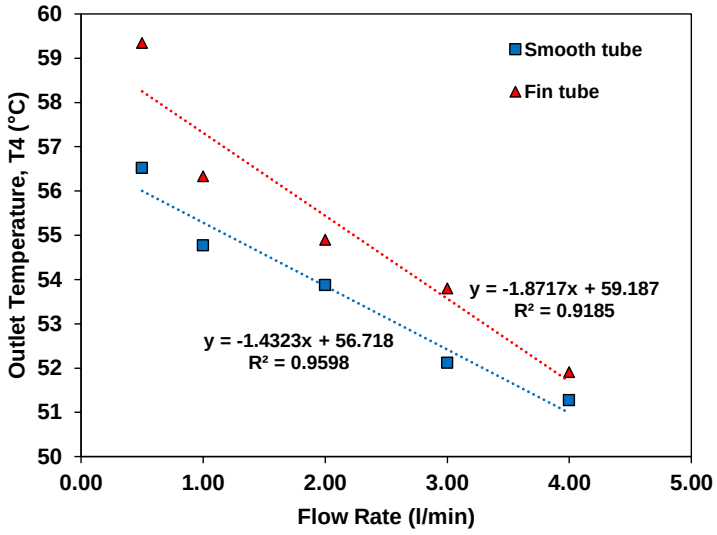

Figure 12. Variation of maximum outlet water temperature with flow rate.

Table 6. Outlet water temperature for smooth and fins absorber tubes.

Flow rate (Liters per minute)	Maximum water temperature smooth tube. (°C)	Maximum water temperature fins tube. (°C)	Difference (°C)	Difference (%)
0.5	56.52	59.34	2.82	4.75
1.0	54.77	56.33	1.56	2.77
2.0	53.87	54.90	1.03	1.88
3.0	52.12	53.80	1.68	3.12
4.0	51.27	51.91	0.64	1.23

Figure 13 shows the series of increasing temperatures. ('Temperature Difference') at each point in the absorption tube: T_2-T_1, T_3-T_2, T_4-T_3, and T_4-T_1. It can be seen that the total number of temperature differences 'T_2-T_1' + 'T_3-T_2' + 'T_4-T_3' is equal to the temperature difference between temperature sensors i.e., T_1-T_4. There is a significant temperature difference between T_2 and T_1, compared to points T_2 and T_3 as well as T_3 and T_4. This is due to the flow passing through the insulation before entering the absorber tube, which causes a significant difference in the early stages. However, when the flow passes through the absorber tube, the flow conditions become more similar, resulting in a lower temperature change in the subsequent period. Results are plotted at different flow rates for smooth and fins copper tubes. As expected, the temperature difference decreases with an increase in flow rate, achieving a maximum temperature difference at 0.5 liters per minute. It was also found that the temperature difference for the fins tube was higher than for smooth copper tubes, which is true at all flow rates. This is due to the greater heat-absorbing area of the fins tube. This is consistent with several research publications [29, 30, 70]. Furthermore, the length of the SPT collector affects the temperature difference. Therefore, a longer system will enhance the overall efficiency albeit at the expense of more pumping power due to greater friction losses.

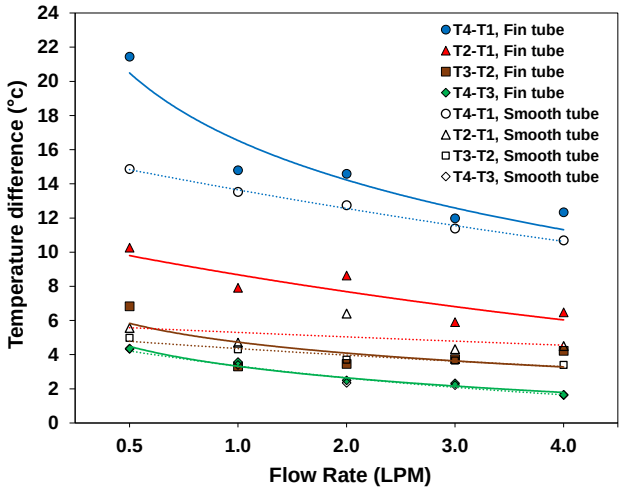

Figure 13. Water heating in the collector at different flow rates.

3.3. Useful Energy

Figure 14 shows heat transfer as a function of water flow rates for smooth and fins copper tubes. It can be seen that the heat transfer rate in the smooth absorber tubes is almost constant for all flow rates however, there is a significant difference in the fins absorber tube especially at lower flow rate. The results showed that fins tubes achieved a heat transfer rate of 1375.55 W at a low flow rate of 0.5 liters per minute, more than smooth tubes of 43.94% at the same flow rate. This is because the surface area for absorbing the

solar radiation is much larger (due to the fins) than the surface for heat transfer between the working fluid and the tube. The results therefore suggest that externally fins tube absorbers need to be operated at low flow rates to maximize the useful energy. Similarly, this illustrates the need for modelling the heat transfer in this sort of system giving the fact that conventional correlations are unlikely to be applicable.

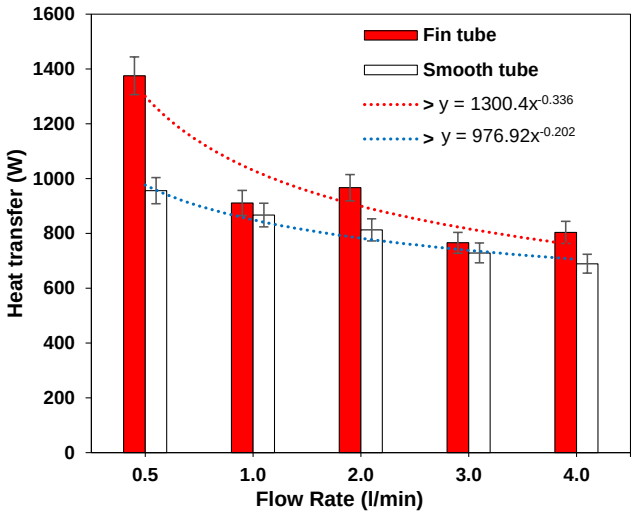

Figure 14. Heat transfer is a function of flow rate for absorber tubes with and without fins.

3.4. Efficiency

Figure 15 shows the thermal efficiency of the SPT collector as a function of water flow rate for smooth and fins absorber tubes. Overall efficiency is computed based on the thermal energy generated from a solar receiver compared with solar irradiation. It can be seen that a flow rate of 0.5 liters per minute gives the maximum efficiency of 18.2% and 12.3% for fins and smooth tubes, respectively. This trend is likely due to increased heat losses at higher flow rates. Furthermore, it can be observed that efficiency is consistently less than 20%, which is well below an expected efficiency of more than 40% [30, 71]. However, there are many factors that can contribute to low efficiency. For example, this low-cost collector was invented using local skills and materials, as well as the refraction of sunlight, control mechanisms, and movement mechanisms of the system, particularly the accuracy of tracking the solar path of the sun by the sun-tracking system, which will result in lower efficiency.

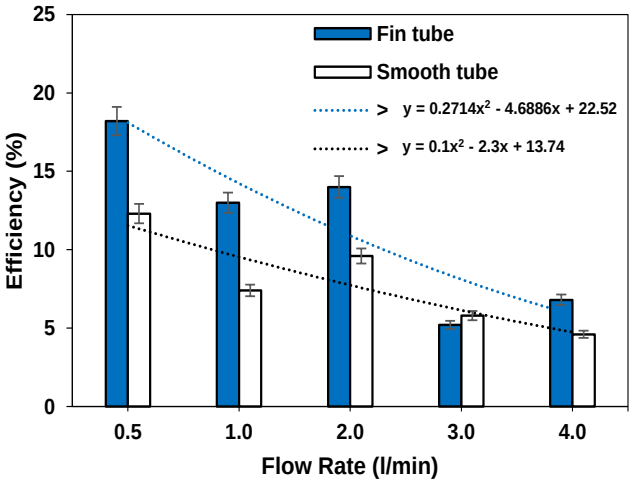

Figure 15. Thermal efficiency of fins and smooth absorber tubes as a function of water flow rate.

The ASHRAE standard 93 (2003) [72] was used to estimate the thermal efficiency of the SPT in terms of input temperature and ambient temperature during steady-state conditions. Equation (25) [73] shows that overall thermal efficiency

$$\eta = F_R \eta_o - \frac{F_R U_L}{CR}\left(\frac{T_{in}-T_a}{G}\right) \quad (25)$$

Where F_R is the factor of heat removal, η_o is optical efficiency, and U_L is the overall loss coefficient.

The results from the experiment were plotted as SPT efficiency curves using standard least squares technical plotting. The slope is the term "$F_R U_L/CR$", and the intercept is the term "$F_R \eta_o$". From Figure 16, it can be seen that the slope is 0.027 and the intercept is 0.186. Therefore, the equation for the overall thermal efficiency of the solar parabolic trough collector can be rewritten as equation (26).

$$\eta = 0.186 - 0.027\left(\frac{T_{in}-T_a}{G}\right) \quad (26)$$

Figure 16 presents a thermal performance curve based on the data collected throughout the experiment. The line of the least-squares fit equation is shown in the graph and indicates that the collector has an intercept efficiency of about 18%, which is much lower than expected, as established in earlier studies [74-76] and reduces with flow rate. It can be observed that as the mass flow rate increases, the term "$(T_{in}-T_a)/G$" increases, resulting in a decrease in efficiency. Therefore, it can be seen that the change in efficiency depends on the parameter of the temperature difference in the term "$(T_{in}-T_a)/G$".

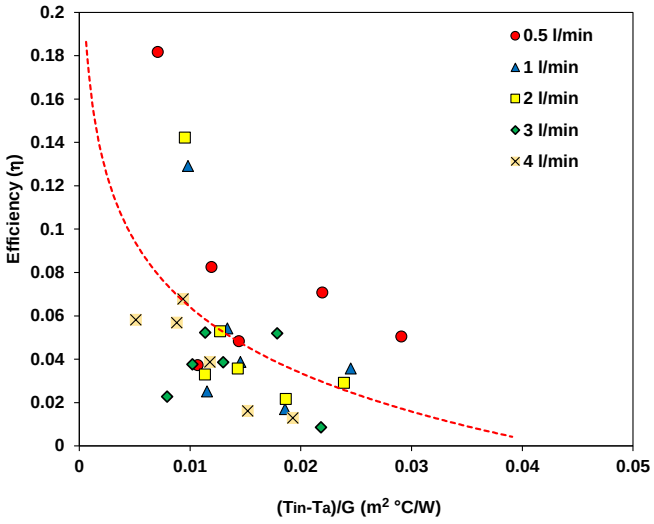

Figure 16. Efficiency of the SPT with fins absorber tube at various flow rates. Least-squares fit line shown.

Figure 17 shows that a copper tube with external fins consistently outperforms the smooth tube of a solar receiver. The trend of efficiency with the term "$(T_{in}-T_a)/G$" observed in this study is similar to earlier research [75-77]. It can be observed that the efficiency is much higher at lower values of the term "$(T_{in}-T_a)/G$", which further supports the suggestion that the lower performance at higher flow rates is as a result of increased heat losses. This is because the losses will be proportional to the temperature difference between the fluid and the ambient air. Additionally, Table 7 compares the efficiency and heat transfer parameters for both cases, fins and smooth tube. The fins solar absorber tube is about 48% more efficient than the smooth tube mainly due to improved energy absorption.

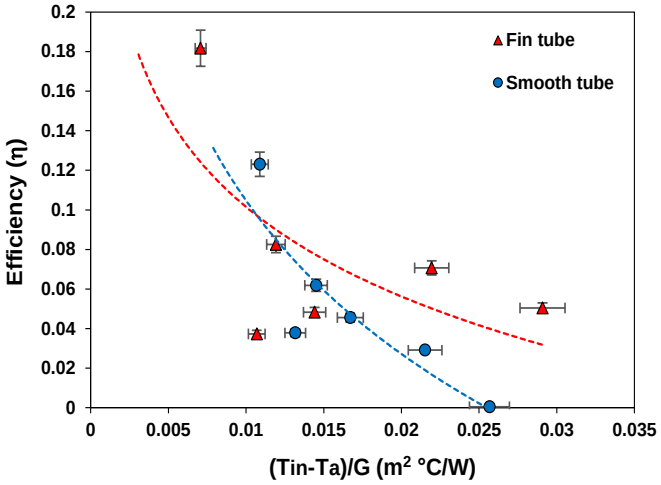

Figure 17. The efficiency of the SPT with reduced temperature for absorber tubes with and without fins at a flow rate of 0.5 liters per minute.

Table 7. The comparison results of efficiency and heat transfer parameters for both cases.

Cases	Heat transfer. (W)	Maximum efficiency. (%)	Equation
Fins tube	1375.55	18.20	y = -0.065ln(x) - 0.1991
Smooth tube	955.65	12.30	y = -0.112ln(x) - 0.4105

3.5. Environmental Impact Evaluation

In Thailand, fossil fuels account for 91.5% of the nation's total power generation. Natural gas makes up more than 70% of these fossil fuels [78-80]. As a result, the objective can be achieved through CO_2 reduction at the point of origin, which is power generation using fossil fuels. Because these fossil fuels are the main source of CO_2 emissions (CO_2e) [79], In terms of the environmental study, this solar parabolic trough system doesn't release carbon dioxide (CO_2) because it doesn't use fossil fuels to generate heat power. From equation (27) [19, 81], you can figure out how to figure out how much carbon dioxide (CO_2) is released during the process of making energy from the parabolic system.

$$CO_2 emissions = Activity\ Data\ (from\ SPT) \times Emissions\ Factor \quad (27)$$

Where CO_2 emissions (CO_2e) are expressed in kg, the emission factor is equal to 0.5986 $kgCO_2e/kWh$ [80] for Thailand in this case study.

Figure 18 shows the reduction in CO_2 emissions rate when using the SPT system as a function of water flow rate for smooth and fins copper tubes. It can be seen that the rate of CO_2 emissions reduction is significantly different in the fins adsorbent tube. especially at lower flow rates. The results showed that fins tubes reduced CO_2 emissions by 0.2726 Metric tons of CO_2e per year at a low flow rate of 0.5 liters per minute, more than smooth tubes, which reduced emissions by 43.92% (Table 8) at the same flow rate. This is because fins tubes generate more heat energy. Similarly, the results suggest that external fins tube adsorbers need to operate at low flow rates to maximize useful energy. Additionally, Table 8 compares Using a SPT system with fins and smooth tubes at a flow rate of 0.5 l/min for both types reduce the rate of CO_2 emissions. As a result, the fins solar absorber tube is about 43.92% more efficient than the smooth tube at reducing CO_2 emissions. That shows that the STP systems can help avoid CO emissions equivalent (CO_2e), which has made it known that the STP systems are more environmentally friendly.

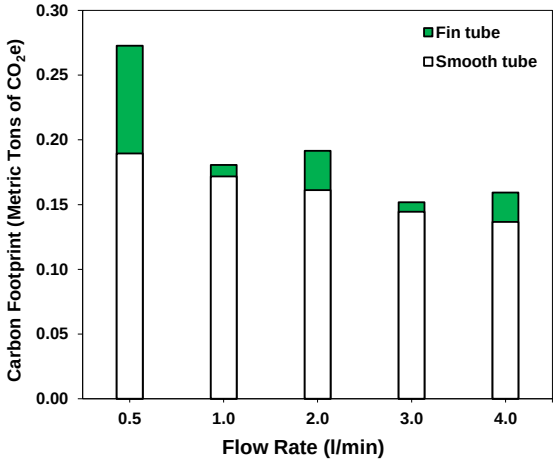

Figure 18. The avoided CO_2 emissions rate as a function of flow rate for using a SPT system.

Table 8. The avoided CO_2 emissions rate is achieved by using a SPT system for both cases at a flow rate of 0.5 l/min.

Cases	Energy (kWh/day)	Carbon Footprint (Metric Tons of CO_2e/day)	Carbon Footprint (Metric Tons of CO_2e/year)	Rate increase. (%)
Fins tube	1.376	0.0007	0.2726	43.92
Smooth tube	0.956	0.0005	0.1894	-

3.6. Cost analysis of the solar parabolic trough system projects

This SPT system was designed and constructed in Thailand for this case study. The duration of the project is 20 years. The total initial investment cost is 10,526.32 USD at an interest rate of 6.75%. From Table 9, the project's financial analysis results show that the net present value (*NPV*) is 988.87 USD, which is greater than zero. The internal rate of return (*IRR*) is 9.57%, which is higher than the loan rate. Or the specified discount rate is 6.75% and the payback period is approximately 8.77 years, which is within the project's implementation period. Consequently, when comparing the study results with investment decision criteria, the project is worth the investment.

Table 9. Economic results for the solar parabolic trough system (for this case study).

Energy (kWh/day)	Annual Energy (kWh/year)	Initial investment (USD)	Year investor IRR achieved (year)	interest rate (%)[63]	Weighted average cost of capital, WACC (%)[82]	Net present value, NPV (USD)	Internal rate of return, IRR (%)	Payback period, PB (year)
1.376	502.24	10,526.32	20	6.75	8.31	988.87	9.57	8.77

4. Conclusions

This paper compares the thermal performance of smooth and external fins absorber tubes for parabolic trough collectors. The SPT, with a focal length of 300 mm and a length of 5.1 m, was designed and built to test its ability to generate heat, using water as a heat transfer fluid at flow rates ranging from 0.5 to 4 liters per minute. The water was circulated through solar absorber tubes, with and without external fins, which were placed at the focal point of the parabolic trough. The conclusions from the study include:

1. The results showed that the external fins absorber tube has the potential to improve thermal efficiency by up to 48% compared to the smooth absorber tube. This was attributed to the fact that the outer surface has more area for energy absorption.

2. The external fins absorber tube provides a higher exit temperature than the smooth absorber tube at the same flow rate. With a flow rate of 0.5 liters per minute, the maximum output temperature from the fins tube is 59.34 °C; this is 2.82 °C more than for the smooth copper pipe, representing a 4.75% increase.
3. The results showed that at a low flow rate of 0.5 liters per minute, fins tubes achieved a heat transfer rate of 1375.55 W, more than smooth tubes at 43.94%, and efficiency at 18.2% that more than smooth tubes at around 48%.
4. The research found that the fins tubes of the SPT system avoided CO_2 emissions by 0.2726 metric tons of CO_2e per year, with fins tubes outperforming smooth tubes by 43.92% at a flow rate of 0.5 liters per minute.
5. The main conclusion of the paper is that external fin absorber tubes are a less expensive and easier-to-manufacture method of improving the thermal performance of SPT.

For future work, it is recommended to study parameters for optimizing the geometry of fins such as shapes, widths, thicknesses, and spaces between each fin, including reflector sheets at both ends of the solar collector. Numerical analyses could be carried out to optimize geometrical characteristics, which will reduce time and experimental validation costs.

Author Contributions: Conceptualization, T.L. and M.O.; methodology, T.L. and M.O.; investigation, T.L., M.O. and D.H.; resources, T.L., N.P. and P.B.; data curation, T.L.; writing—original draft preparation, T.L., M.O. and D.H.; writing—review and editing, T.L., M.O., D.H., N.P. and P.B.; supervision, M.O. and D.H.; All authors have read and agreed to the published version of the manuscript.

Data Availability Statement: Not applicable.

Acknowledgments: The authors would like to acknowledge Mr Tirarut Eaumkeb, Mr Satawat Udnoonchart and technical staff from the Department of Mechanical Engineering, Faculty of Engineering, Srinakharinwirot University, Nakhornayok, Thailand, for their assistance in this work.

Conflicts of Interest: The authors declare no conflict of interest.

Appendix A

Figure A1 shows all data on solar radiation collected on clear and cloudy days throughout the experiment. It can be seen that the experimental data collection was conducted for 20 days. However, 10 days of the data with the fewest cloudy days were used for the analysis, as shown in Figure 10.

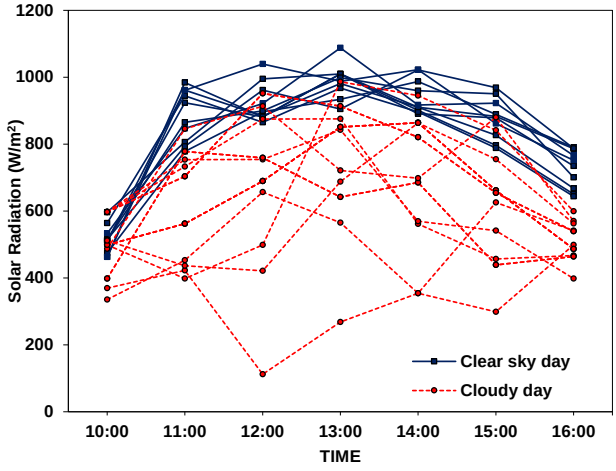

Figure A1. The collection of data on the variation of solar radiation with time on clear and cloudy days.

Nomenclature

A_a	[m²]	Aperture area
A_r	[m²]	Receiver area surface
A_c	[m²]	Cross sectional area of copper tube
C_p	[J/kg.K]	Specific heat capacity
CR	[-]	The geometric concentration ratio
D	[m]	Characteristic diameter dimension
D_{go}	[m]	Outside diameter of glass envelope
D_{gi}	[m]	Inner glass cover diameter
D_{ci}	[m]	Inside diameter of copper tube
D_{co}	[m]	Outside diameter of copper tube
E	[hrs]	Equation of time
F_R	[-]	The factor of heat removal
f	[-]	Focus of parabolic
G	[W/m²]	Solar radiation
h	[W/m²K]	The heat transfer coefficient
k	[W/(m.K)	Thermal conductivity
Re	[-]	Reynolds number
st	[-]	Local standard time
I_b	[W/m²]	The direct solar light intensity
I_{eff}	[W/m²]	The effective intensity of sunlight
L	[m]	Characteristic linear dimension
L_r	[m]	Receiver length
$Long$	[-]	Longitude
l	[-]	The latitudes on the Earth
$\dot{m}$	[kg/s]	Mass flow rate of fluid flow
m	[kg]	Mass of fluid
n	[day]	The year's day
N	[-]	North
S	[-]	South
Re	[-]	Reynolds number
Q	[W]	Thermal power to fluid
Q_{water}	[W]	Daily energy gained by water
Q_s	[W]	Solar energy on the trough aperture
q	[W/m²]	Heat flux density
T	[°C]	Temperature
t	[s]	Time
U_L	[W/m²K]	Overall heat loss coefficient
v	[m/s]	Flow speed of fluid
$\dot{V}$	[m³/s]	Volumetric flow rate
P	[-]	The position of a point on the earth's surface
x	[m]	The distance of the parabolic curve along the X-axis
Y_z	[-]	Accuracy of the devices
y	[m]	Curve length of the parabolic
W	[m]	The width of the parabolic collector

Special characters

ω	[°]	The angle of each hour
δ	[°]	The sun's declination angle
θ	[°]	The sun's incident angle
η	[-]	Overall efficiency
η_o	[-]	Optical efficiency
ρ	[kg/m³]	Density of the fluid
α		Reflectance of reflector surface
μ	[kg/(m.s)	Dynamic viscosity of the fluid

Subscripts

st	Longitude drags through the standard time
s	Solar
r	Receiver tube
fm	Mean fluid temperature
$final$	Final water temperature of system
$initial$	Initial water temperature of system
Loc	Longitude drags through the local time
u	Useful

1-4	Position temperature
in	Inlet fluid temperature
out	Outlet fluid temperature
a	Ambient temperature
g	Glass receiver tube
t	Water tank temperature
Abbreviations	
AT	Absorber Tube
ASHRAE	American Society of Heating, Refrigerating and Air-Conditioning Engineers
CLFR	Compact Linear Fresnel Reflector
HTF	The Heat Transfer Fluid
IRR	The Internal Rate of Return
NPV	The Net Present Value
PB	Payback Period
PDC	Parabolic Dish Collector
SPT	Solar Parabolic Trough
SPTC	Solar Parabolic Trough Collector
SWU	Srinakharinwirot University
USD	The currency abbreviation for the U.S. dollar
UTC	Coordinated Universal Time

References

1. Balakrishnan, P., et al., *Current status and future prospects of renewable energy: A case study.* Energy Sources, Part A: Recovery, Utilization, and Environmental Effects, 2020. **42**(21): p. 2698-2703.
2. Bamisile, O., et al., *A review of renewable energy potential in Nigeria; solar power development over the years.* Engineering and Applied Science Research, 2017. **44**(4): p. 242-248.
3. Garg, H., *Solar energy: fundamentals and applications*. 2000: Tata McGraw-Hill Education.
4. Kabir, E., et al., *Solar energy: Potential and future prospects.* Renewable and Sustainable Energy Reviews, 2018. **82**: p. 894-900.
5. Khan, B., *Non-conventional energy resources*. 2006: Tata McGraw-Hill Education.
6. Rai, G., *Non conventional Energy sources Khanna Publishers*. 1986, Delhi.
7. Krungkaew, S., et al., *Costs and benefits of using parabolic greenhouse solar dryers for dried herb products in Thailand.* GEOMATE Journal, 2020. **18**(67): p. 96-101.
8. Duffie, J.A., W.A. Beckman, and N. Blair, *Solar engineering of thermal processes, photovoltaics and wind*. 2020: John Wiley & Sons.
9. Badran, O., *Study in industrial applications of solar energy and the range of its utilization in Jordan.* Renewable Energy, 2001. **24**(3-4): p. 485-490.
10. Schiel, W. and T. Keck, *Parabolic dish concentrating solar power systems*, in *Concentrating solar power technology*. 2021, Elsevier. p. 311-355.
11. Price, H., et al. *Field survey of parabolic trough receiver thermal performance*. in *International Solar Energy Conference*. 2006.
12. Romero, M. and A. Steinfeld, *Concentrating solar thermal power and thermochemical fuels.* Energy & Environmental Science, 2012. **5**(11): p. 9234-9245.
13. Gong, J.-h., et al., *Improving the performance of large-aperture parabolic trough solar concentrator using semi-circular absorber tube with external fin and flat-plate radiation shield.* Renewable Energy, 2020. **159**: p. 1215-1223.
14. Gong, J.-h., et al., *Comparative study of heat transfer enhancement using different fins in semi-circular absorber tube for large-aperture trough solar concentrator.* Renewable Energy, 2021. **169**: p. 1229-1241.
15. Shayan, M.E., G. Najafi, and F. Ghasemzadeh, *Advanced study of the parabolic trough collector using aluminum (III) oxide.* International Journal of Smart Grid, 2020. **4**(3): p. 111-116.
16. Bi, Y., et al., *Performance analysis of solar air conditioning system based on the independent-developed solar parabolic trough collector.* Energy, 2020. **196**: p. 117075.
17. Kumar, D. and S. Kumar, *Analytical performance investigation of parabolic trough solar collector with computed optimum air gap.* International Journal of Energy and Environment, 2015. **6**(1): p. 87.
18. Aseri, T.K., C. Sharma, and T.C. Kandpal, *Estimation of capital costs and techno-economic appraisal of parabolic trough solar collector and solar power tower based CSP plants in India for different condenser cooling options.* Renewable Energy, 2021. **178**: p. 344-362.
19. Praveenkumar, S., et al., *Techno-economics and the identification of environmental barriers to the development of concentrated solar thermal power plants in India.* Applied Sciences, 2022. **12**(20): p. 10400.
20. Purohit, I. and P. Purohit, *Techno-economic evaluation of concentrating solar power generation in India.* Energy policy, 2010. **38**(6): p. 3015-3029.
21. Tahir, S., et al., *Techno-economic assessment of concentrated solar thermal power generation and potential barriers in its deployment in Pakistan.* Journal of Cleaner Production, 2021. **293**: p. 126125.
22. Boretti, A., *Cost and production of solar thermal and solar photovoltaics power plants in the United States.* Renewable Energy Focus, 2018. **26**: p. 93-99.

23. PRESSEBOX. *The first parabolic trough plant using direct steam generation – delivers its full 5 MW of output to Thailand's power network*. 2023 [cited 2023 04/03]; Available from: https://www.pressebox.com/pressrelease/solarlite-gmbh-duckwitz/TSE-1-The-first-parabolic-trough-plant-using-direct-steam-generation-delivers-its-full-5-MW-of-output-to-Thailands-power-network/boxid/478604.
24. Fuqiang, W., et al., *Parabolic trough receiver with corrugated tube for improving heat transfer and thermal deformation characteristics.* Applied energy, 2016. **164**: p. 411-424.
25. Huang, Z., et al., *Numerical investigations on fully-developed mixed turbulent convection in dimpled parabolic trough receiver tubes.* Applied Thermal Engineering, 2017. **114**: p. 1287-1299.
26. Huang, Z., et al., *Numerical study on heat transfer enhancement in a receiver tube of parabolic trough solar collector with dimples, protrusions and helical fins.* Energy Procedia, 2015. **69**: p. 1306-1316.
27. Peng, H., et al., *Performance analysis of absorber tube in parabolic trough solar collector inserted with semi-annular and fin shape metal foam hybrid structure.* Case Studies in Thermal Engineering, 2021. **26**: p. 101112.
28. Vengadesan, E., et al., *Experimental study on heat transfer enhancement of parabolic trough solar collector using a rectangular channel receiver.* Journal of the Taiwan Institute of Chemical Engineers, 2022. **135**: p. 104361.
29. Zhao, Z., et al., *Experimental study of pin finned receiver tubes for a parabolic trough solar air collector.* Solar Energy, 2020. **207**: p. 91-102.
30. Bellos, E., C. Tzivanidis, and D. Tsimpoukis, *Multi-criteria evaluation of parabolic trough collector with internally finned absorbers.* Applied Energy, 2017. **205**: p. 540-561.
31. Jathar, L.D., et al., *Effect of various factors and diverse approaches to enhance the performance of solar stills: a comprehensive review.* Journal of Thermal Analysis and Calorimetry, 2021: p. 1-32.
32. Tayebi, R., S. Akbarzadeh, and M.S. Valipour, *Numerical investigation of efficiency enhancement in a direct absorption parabolic trough collector occupied by a porous medium and saturated by a nanofluid.* Environmental Progress & Sustainable Energy, 2019. **38**(2): p. 727-740.
33. Atchuta, S., S. Sakthivel, and H.C. Barshilia, *Selective properties of high-temperature stable spinel absorber coatings for concentrated solar thermal application.* Solar Energy, 2020. **199**: p. 453-459.
34. Joly, M., et al., *Novel black selective coating for tubular solar absorbers based on a sol–gel method.* Solar energy, 2013. **94**: p. 233-239.
35. Kasaeian, A., S. Daviran, and R.D. Azarian, *Optical and thermal investigation of selective coatings for solar absorber tube.* International Journal of Renewable Energy Research (IJRER), 2016. **6**(1): p. 15-20.
36. Fedkin, M. *Parabolic Dish CSP Technology*. 2020 [cited 2022 04/26]; Available from: https://www.e-education.psu.edu/eme812/node/648.
37. Natarajan, S.K., et al., *Experimental analysis of a two-axis tracking system for solar parabolic dish collector.* International Journal of Energy Research, 2019. **43**(2): p. 1012-1018.
38. Wang, K., et al., *Multi-objective optimization of the solar absorptivity distribution inside a cavity solar receiver for solar power towers.* Solar energy, 2017. **158**: p. 247-258.
39. Naphon, P., *Experimental investigation the nanofluids heat transfer characteristics in horizontal spirally coiled tubes.* International Journal of Heat and Mass Transfer, 2016. **93**: p. 293-300.
40. Navakrishnan, S., et al., *An experimental study on simultaneous electricity and heat production from solar PV with thermal energy storage.* Energy Conversion and Management, 2021. **245**: p. 114614.
41. Ghasemi, S.E. and A.A. Ranjbar, *Numerical thermal study on effect of porous rings on performance of solar parabolic trough collector.* Applied Thermal Engineering, 2017. **118**: p. 807-816.
42. Reddy, K., K.R. Kumar, and C. Ajay, *Experimental investigation of porous disc enhanced receiver for solar parabolic trough collector.* Renewable Energy, 2015. **77**: p. 308-319.
43. Zheng, Z., Y. Xu, and Y. He, *Thermal analysis of a solar parabolic trough receiver tube with porous insert optimized by coupling genetic algorithm and CFD.* Science China Technological Sciences, 2016. **59**(10): p. 1475-1485.
44. Mwesigye, A., T. Bello-Ochende, and J.P. Meyer, *Heat transfer and entropy generation in a parabolic trough receiver with wall-detached twisted tape inserts.* International Journal of Thermal Sciences, 2016. **99**: p. 238-257.
45. Song, X., et al., *A numerical study of parabolic trough receiver with nonuniform heat flux and helical screw-tape inserts.* Energy, 2014. **77**: p. 771-782.
46. Zhu, X., L. Zhu, and J. Zhao, *Wavy-tape insert designed for managing highly concentrated solar energy on absorber tube of parabolic trough receiver.* Energy, 2017. **141**: p. 1146-1155.
47. Chakraborty, O., et al., *Effects of helical absorber tube on the energy and exergy analysis of parabolic solar trough collector–A computational analysis.* Sustainable Energy Technologies and Assessments, 2021. **44**: p. 101083.
48. Muñoz, J. and A. Abánades, *Analysis of internal helically finned tubes for parabolic trough design by CFD tools.* Applied energy, 2011. **88**(11): p. 4139-4149.
49. Valizade, M., M. Heyhat, and M. Maerefat, *Experimental study of the thermal behavior of direct absorption parabolic trough collector by applying copper metal foam as volumetric solar absorption.* Renewable Energy, 2020. **145**: p. 261-269.
50. Guerraiche, D., et al., *Experimental and numerical study of a solar collector using phase change material as heat storage.* Journal of Energy Storage, 2020. **27**: p. 101133.
51. Kaloudis, E., E. Papanicolaou, and V. Belessiotis, *Numerical simulations of a parabolic trough solar collector with nanofluid using a two-phase model.* Renewable Energy, 2016. **97**: p. 218-229.

52. Tripathy, A.K., et al., *Structural analysis of absorber tube used in parabolic trough solar collector and effect of materials on its bending: A computational study.* Solar Energy, 2018. **163**: p. 471-485.
53. Abed, N., et al., *Thermal performance evaluation of various nanofluids with non-uniform heating for parabolic trough collectors.* Case Studies in Thermal Engineering, 2020. **22**: p. 100769.
54. Subramani, J., P. Sevvel, and S. Srinivasan, *Influence of CNT coating on the efficiency of solar parabolic trough collector using AL2O3 nanofluids-a multiple regression approach.* Materials Today: Proceedings, 2021. **45**: p. 1857-1861.
55. Teerapath Limboonruang, N.P., Muyiwa Oyinlola, *Experimental investigation of a locally fabricated low-cost solar parabolic trough in Thailand*, in *16th International conference on heat transfer (HEFAT-ATE 2022)*. 2022: Amsterdam, Netherlands. p. 432-437.
56. Kalogirou, S.A., *Solar energy engineering: processes and systems*. 2013: Academic press.
57. Lüpfert, E., et al. *Toward standard performance analysis for parabolic trough collector fields*. in *SolarPACES Conference Proceedings*. 2004.
58. Zou, B., et al., *An experimental investigation on a small-sized parabolic trough solar collector for water heating in cold areas.* applied energy, 2016. **163**: p. 396-407.
59. Tzivanidis, C., et al., *Thermal and optical efficiency investigation of a parabolic trough collector.* Case Studies in Thermal Engineering, 2015. **6**: p. 226-237.
60. Sookramoon, K. *Design, constructand performance evaluation of a 2-stage parabolic through solar concentrator in PathumThani*. in *Advanced Materials Research*. 2014. Trans Tech Publ.
61. Ayodele, T., et al., *Optimal design of wind-powered hydrogen refuelling station for some selected cities of South Africa.* International Journal of Hydrogen Energy, 2021. **46**(49): p. 24919-24930.
62. Brigham, E.F. and J.F. Houston, *Fundamentals of financial management: Concise*. 2021: Cengage Learning.
63. Intaraburt, W., et al., *Feasibility Study of Water Reclamation Projects in Industrial Parks Incorporating Environmental Benefits: A Case Study in Chonburi, Thailand.* Water, 2022. **14**(7): p. 1172.
64. Praveenkumar, S., et al., *experimental study on performance enhancement of a photovoltaic module incorporated with CPU heat pipe—A 5E analysis.* Sensors, 2022. **22**(17): p. 6367.
65. Janjai, S., *A method for estimating direct normal solar irradiation from satellite data for a tropical environment.* Solar energy, 2010. **84**(9): p. 1685-1695.
66. Janjai, S., J. Laksanaboonsong, and T. Seesaard, *Potential application of concentrating solar power systems for the generation of electricity in Thailand.* Applied Energy, 2011. **88**(12): p. 4960-4967.
67. Oyinlola, M. and G. Shire, *Characterising micro-channel absorber plates for building integrated solar thermal collectors.* Building Services Engineering Research and Technology, 2019. **40**(1): p. 13-29.
68. Oyinlola, M.A., G.S. Shire, and R. Moss, *Thermal analysis of a solar collector absorber plate with microchannels.* Experimental Thermal and Fluid Science, 2015. **67**: p. 102-109.
69. Ali, Z., et al., *Insight into the dynamics of Oldroyd-B fluid over an upper horizontal surface of a paraboloid of revolution subject to chemical reaction dependent on the first-order activation energy.* Arabian Journal for Science and Engineering, 2021. **46**(6): p. 6039-6048.
70. Amina, B., et al., *Heat transfer enhancement in a parabolic trough solar receiver using longitudinal fins and nanofluids.* Journal of thermal science, 2016. **25**(5): p. 410-417.
71. Norouzi, A.M., et al., *Experimental study of a parabolic trough solar collector with rotating absorber tube.* Renewable Energy, 2021. **168**: p. 734-749.
72. Standard, A., *93 (2003) Method of testing to determine the thermal performance of solar collectors. American Society of Heating.* Refrigeration and Air Conditioning Engineers, Atlanta, GA. **30329**.
73. Arasu, A.V. and T. Sornakumar, *Design, manufacture and testing of fiberglass reinforced parabola trough for parabolic trough solar collectors.* Solar Energy, 2007. **81**(10): p. 1273-1279.
74. Yousefi, T., et al., *An experimental investigation on the effect of MWCNT-H2O nanofluid on the efficiency of flat-plate solar collectors.* Experimental Thermal and Fluid Science, 2012. **39**: p. 207-212.
75. Yousefi, T., et al., *An experimental investigation on the effect of Al2O3–H2O nanofluid on the efficiency of flat-plate solar collectors.* Renewable Energy, 2012. **39**(1): p. 293-298.
76. Zamzamian, A., et al., *An experimental study on the effect of Cu-synthesized/EG nanofluid on the efficiency of flat-plate solar collectors.* Renewable Energy, 2014. **71**: p. 658-664.
77. Jamal-Abad, M.T., S. Saedodin, and M. Aminy, *Experimental investigation on a solar parabolic trough collector for absorber tube filled with porous media.* Renewable Energy, 2017. **107**: p. 156-163.
78. Agency, I.E., *Thailand Electricity Security Assessment*. 2016: International Energy Agency.
79. Choomkong, A., et al., *A study of CO2 emission sources and sinks in Thailand.* Energy Procedia, 2017. **138**: p. 452-457.
80. Thailand Greenhouse Gas Management Organization, T. *Carbon Footprint for Organization: CFO, Corporate Carbon Footprint: CCF*. 2023 [cited 2023 03/2023]; Available from: http://thaicarbonlabel.tgo.or.th.
81. Aroonsrimorakot, S., et al., *Carbon footprint of faculty of environment and resource studies, Mahidol University, Salaya Campus, Thailand.* APCBEE procedia, 2013. **5**: p. 175-180.
82. Arjharn, W. and P.L. Park, *Study of the economy cost of a small scale biomass power plant for rural communities.* 2007.